Supporting Information

Graphitized Carbon-Coated Vanadium Carbide Nanoboscages Modified by Nickel with Enhanced Electrocatalytic Activity for Hydrogen Evolution in both Acid and Alkaline Solution

Lishan Peng, Jingjun Shen, Ling Zhang, Yao Wang, Rui Xiang, Jing Li, Li Li*, Zidong Wei*

Content:

Experimental Section

Figure S1-8

Table S1-8

Additional References 1-12

Experimental Section

Materials: Ammonium metavanadate (NH_4VO_3), oxalic acid ($H_2C_2O_4 \cdot 2HO$), nickel chloride ($NiCl_2 \cdot 6H_2O$), potassium hydroxide (KOH) and sulfuric acid (H_2SO_4) were purchased from Chengdu Kelong Chemical Reagent Factory (China). Pt/C (20 wt.% Pt on Vulcan XC-72R) and Nafion (5 wt.%) were purchased from Sigma-Aldrich. All chemical reagents used in this experiment were of analytical grade. The water used throughout all experiments was purified through a Millipore system.

Preparation of Ni-VO₂ nanoboscages/Ti (Ni-VO₂/Ti): 1 mmol NH_4VO_3 and 1.2 mmol $H_2C_2O_4 \cdot 2H_2O$ were added into a mixed solution (25 mL H_2O and 10 mL ethanol) to form a uniform yellow solution. After magnetic stirring for 30 min, a certain amount of $NiCl_2 \cdot 6H_2O$ was added into the aboved solution with different atomic ratios to V (Ni:V=0:1, 1:4, 1:2, 1:1, 3:2, 2:1, the samples named as NiV_{0-1}/Ti, NiV_{1-4}/Ti, NiV_{1-2}/Ti, NiV_{1-1}/Ti, NiV_{1-2}/Ti, NiV_{3-2}/Ti, NiV_{2-1}/Ti). Then the obtained solutions were transferred into 40 mL Teflon-lined stainless steel autoclave liners with titanium foil which was pretreated in 3 M HCl for 30min and washed with distilled water (DW) and ethanol. The autoclaves were maintained at 180 °C for 2 h, and then cooled to room temperature naturally. The obtained samples were washed with DW for several time and dried in vacuum at 60 °C.

Preparation of Ni-VC@GC nanoboscages/Ti (Ni-VC@C/Ti): A chemical vapor carbonization was used to convert the Ni-VO NBs/Ti into Ni-VC@CNB/Ti. The aboved Ni-VO NBs/Ti were heated at 5 °C min⁻¹ up to 800 °C for 2 h in a reducing atmosphere composed of 20% CH_4, 10% H_2 and 70% N_2 (100 sccm/min), and then cooled to room temperature in a tube furnace. Thereafter, the products were rinsed with DW and ethanol for several times, and vacuum dried at 60 °C overnight. The preparation of samples with different temperatures follows the same procedures as the above-mentioned using NiV_{1-1}/Ti as precursor but at changed carbonization temperatures. The preparation of samples with different mass ratios of the precursors and carbonization temperatures was the same as that outlined above, except that the mass ratio of

Ni/V or the carbonization temperature was changed. Note that, the sample named Ni-VC$_{1-1}$@C-800 means the Ni-VO$_2$/Ti precursor with the Ni/V=1:1 carbonized at 800 °C.

Preparation of Pt/C electrode: The commercial 20 wt.% Pt/C samples were prepared by ultrasonically mixing 4 mg of the catalyst powder with the mixture of 40 μL 5% Nafion solution, 560 μL ethanol and 400 μL H$_2$O for 15 min to form homogeneous catalyst ink. Next, a certain volume of the ink was carefully dropped onto the clean carbon paper, leading to a desirable catalyst loading of about 1.0 mg cm^{-2}.

General characterizations: The surface morphology and the microstructure of the catalysts were analyzed by X-ray diffraction (XRD-6000, Shimadzu), X-ray photoelectron spectroscopy (XPS, PHI 550 ESCA/SAM), field-emission scanning electron microscopy (FE-SEM, JSM-7800, Japan), and energy dispersive X-ray spectra (EDS, OXFORD Link-ISIS-300), respectively. Transmission electron microscopy (TEM) measurements were made on a Hitachi H-8100 electron microscope (Hitachi, Tokyo, Japan) with an accelerating voltage of 200 kV. The Raman spectra were recorded on the Raman Scattering Spectroscopy (Renishaw 2000 system) with excitation by diode laser (514 nm, laser power of 25 mW) in backscattering geometry.

Electrochemical measurements: Electrochemical measurements were performed in a three-electrode cell system with a CHI660D electrochemical analyzer (CH Instruments, Inc., Shanghai). Sizable and shapeable electrodes can be prepared by simply tailoring the Ti foil, and the obtained Ni-VC@CNB/Ti can be directly used as the working electrode (1 cm^2) without employing extra substrates (e.g., glassy-carbon electrode) or binders (e.g., Nafion). To avoid the deposition of Pt, a carbon rod in parallel orientation to the working electrode was used as the counter electrode with a distance of 1 cm and an Hg/HgO electrode (in alkaline electrolyte) or Ag/AgCl electrode (in acid electrolyte) was used as the reference electrode. The electrolyte (1 M KOH or 0.5 M H$_2$SO$_4$) was degassed by bubbling N$_2$ for at least 30 minutes before the electrochemical measurements. Linear sweep voltammetry (LSV) was performed in N$_2$

saturated aqueous solution with a scan rate of 10 mV s^{-1} in a range from 0 to -0.6 V. Durability test was carried out by cyclic voltammetry (CV) scanning from -0.6 V to 0 vs. RHE for 1000 at a scan rate of 50 mV s^{-1} and i-t curve at current density of 10 mA/cm^2 for over 20 h. In all measurements, the potentials reported in our work were vs. a reversible hydrogen electrode (RHE). The long-term durability test was performed using chronopotentiometric measurements. All currents presented are corrected against ohmic potential drop. The electrochemical surface area (ECSA) of these catalysts were estimated by cyclic voltammetry (CV). CV was performed in the potential range without a redox process from 0.2 to 0.3 V (vs RHE) at varying rates from 10 to 35 mV s^{-1} in 1.0 M KOH and 0.5 M H$_2$SO$_4$. The electrochemical impedance spectroscopy (EIS) measurements were carried out from 100000 to 0.1 Hz in in 1.0 M KOH and 0.5 M H$_2$SO$_4$ at the potential of -0.2 V vs. RHE.
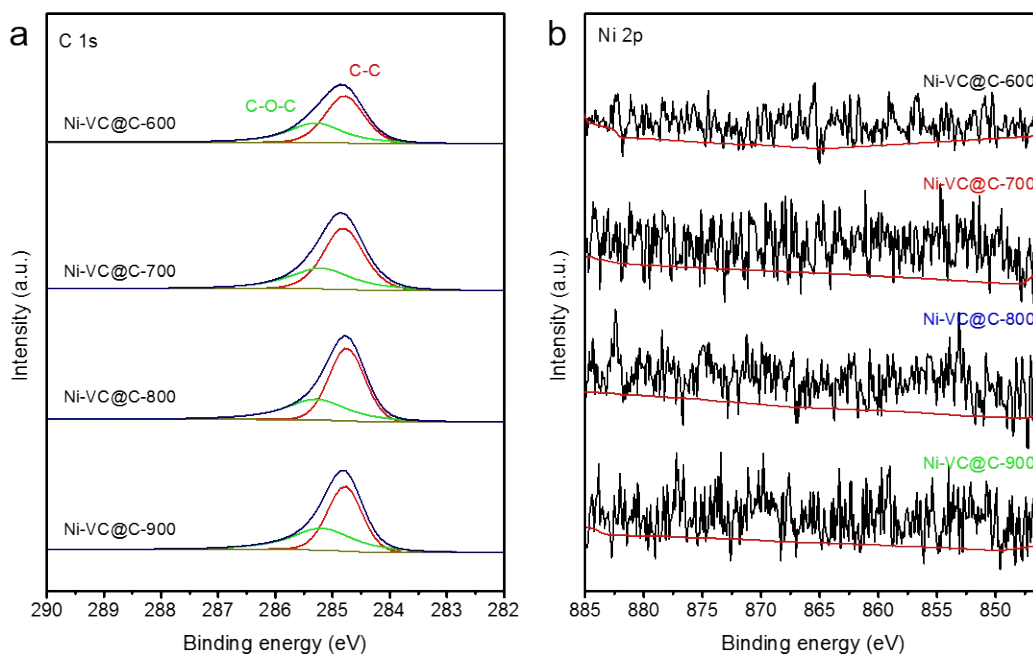
Figure S1. (a) C 1s and (b) Ni 2p XPS spectrums of samples carbonized in different temperatures. The extremely low content of Ni on the surface indicts that most metallic Ni and some vanadium carbides were embedded in carbon, which was also proven by the HR-TEM images (Figure 1).

Table S1. Surface elements contents of the Ni-V samples carbonized in different temperatures.

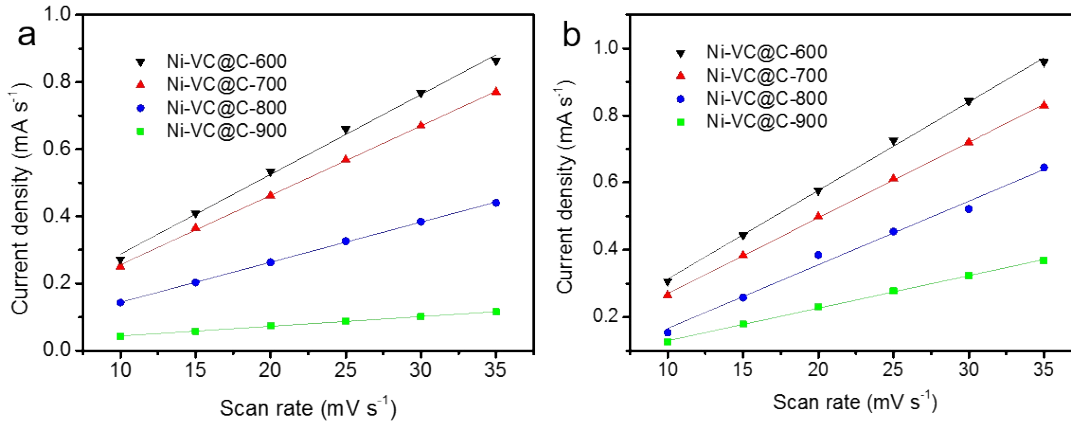| Catalysts	V 2p	Ni 2p[*]	C 1s	O 1s
Ni-VC@C-600	0.99	/	93.01	5.19
Ni-VC@C-700	0.97	/	93.72	4.44
Ni-VC@C-800	0.96	/	95.91	2.22
Ni-VC@C-900	1.48	/	95.57	2.05

[*]Below detection limit.

Figure S2. Estimation of C_{dl} by plotting the current density variation ($\Delta j = (j_a - j_c)/2$) in (a) 0.5 M H_2SO_4 and (b) 1.0 M KOH.

Table S2. Summary of the HER performance in 0.5M H_2SO_4 for samples carbonized in different temperatures.

Catalysts	Onset potential (mV)	Tafel slope (mV dec^1)	Overpotential @10mA/cm^2 (mV)	C_{dl} (mF cm^{-2})
Ni-VC@C-600	235	321	531	23.74
Ni-VC@C-700	82	66	169	20.65
Ni-VC@C-800	47	62	138	11.93
Ni-VC@C-900	209	167	365	2.89

Table S3. Summary of the HER performance in 1.0 M KOH for samples carbonized in different temperatures.

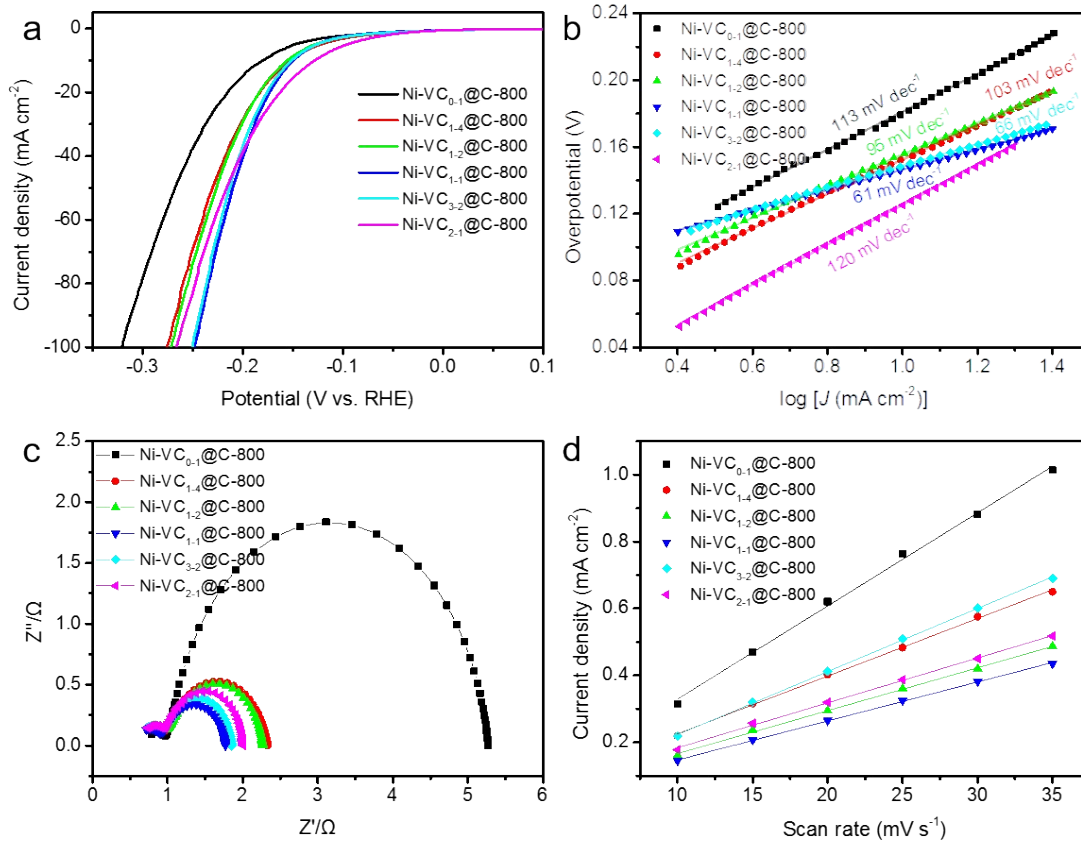| Catalysts	Onset potential (mV)	Tafel slope (mV dec^1)	Overpotential @10mA/cm^2 (mV)	C_{dl} (mF cm^{-2})
Ni-VC@C-600	88	109	208	26.35
Ni-VC@C-700	52	107	172	22.54
Ni-VC@C-800	28	105	146	18.94
Ni-VC@C-900	140	131	504	9.68

Figure S3. (a) Polarization curves and (b) Tafel plots measured in 0.5 M H_2SO_4 for samples carbonized 800°C with different Ni incorporation. (c) Nyquist plots for the corresponding samples measured at a voltage -0.1 V (vs. RHE) over the frequency range 100 KHz to 0.01 Hz in 0.5 M H_2SO_4. (d) Estimation of C_{dl} by plotting the current density variation ($\Delta j = (ja - jc)/2$) in 0.5 M H_2SO_4.

Table S4. Summary of the HER performance in 0.5M H_2SO_4 for samples carbonized 800°C with different Ni incorporation.

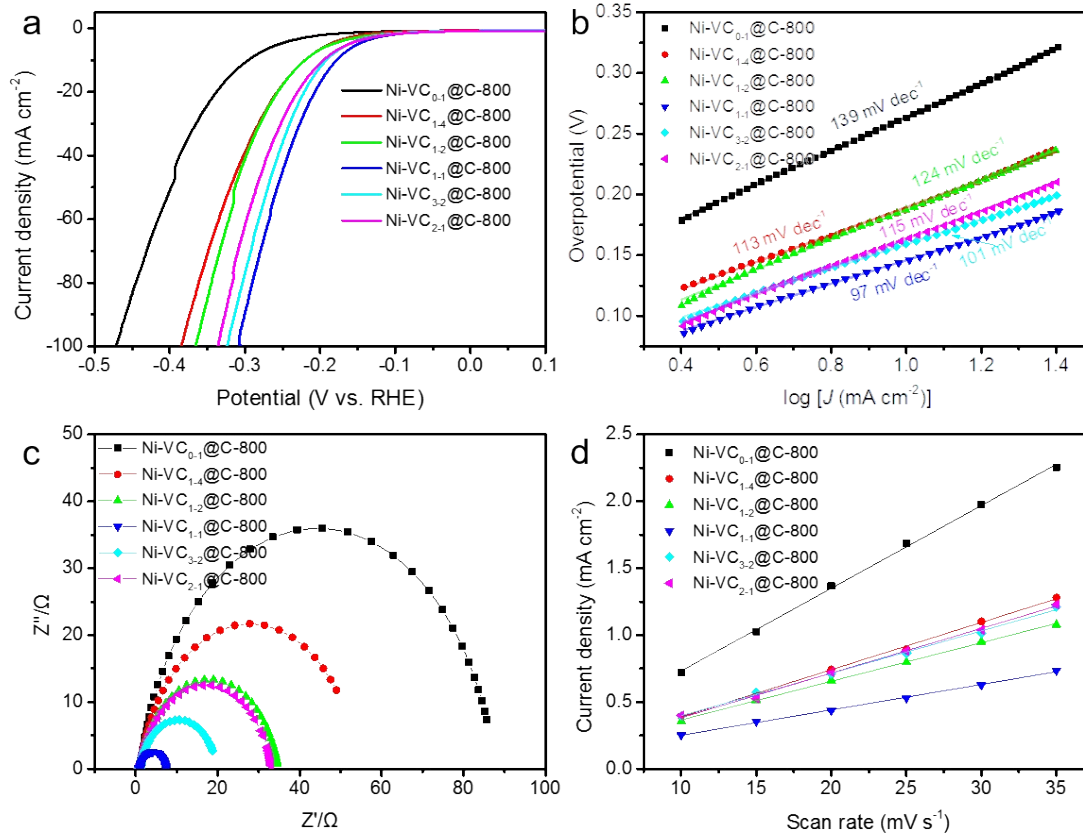| Catalysts	Onset potential (mV)	Tafel slope (mV dec^1)	Overpotential @10mA/cm^2 (mV)	C_{dl} (mF cm^{-2})	Overpotential @10mA/cm^2$_{ECSA}$ (mV)
Ni-VC$_{0-1}$@C-800	42	113	181	27.83	181
Ni-VC$_{1-4}$@C-800	45	103	153	17.21	132
Ni-VC$_{1-2}$@C-800	40	95	156	12.81	125
Ni-VC$_{1-1}$@C-800	47	61	138	11.83	120
Ni-VC$_{3-2}$@C-800	38	65	151	18.87	137
Ni-VC$_{2-1}$@C-800	37	120	128	13.40	109

Figure S4. (a) Polarization curves and (b) Tafel plots measured in 1.0 M KOH for samples carbonized 800°C with different Ni incorporation. (c) Nyquist plots for the corresponding samples measured at a voltage −0.1 V (vs RHE) over the frequency range 100 kHz to 0.01 Hz in 1.0 M KOH. (d) Estimation of C_{dl} by plotting the current density variation ($\Delta j = (j_a - j_c)/2$) in 1.0 M KOH.

Table S5. Summary of the HER performance in 1.0 M KOH for samples carbonized 800°C with different Ni incorporation.

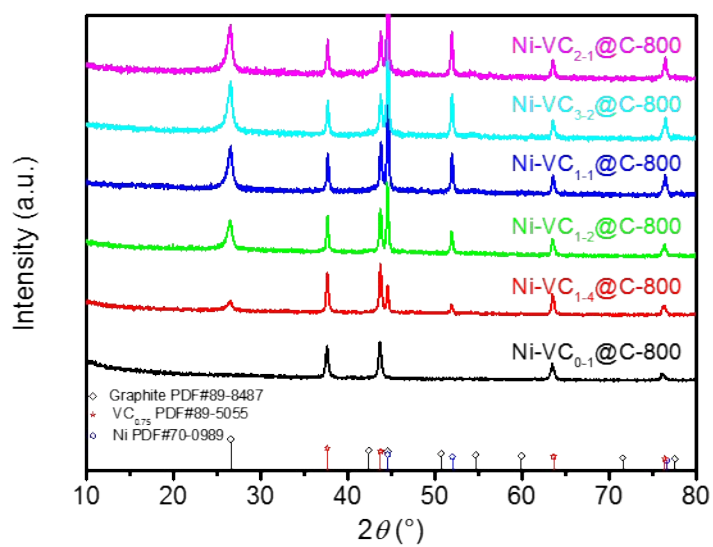| Catalysts	Onset potential (mV)	Tafel slope (mV dec^1)	Overpotential @10mA/cm^2 (mV)	C_{dl} (mF cm^{-2})	Overpotential @10mA/cm$^2_{ECSA}$ (mV)
Ni-VC$_{0-1}$@C-800	98	139	263	61.81	263
Ni-VC$_{1-4}$@C-800	72	113	188	35.33	161
Ni-VC$_{1-2}$@C-800	31	124	188	28.87	147
Ni-VC$_{1-1}$@C-800	26	97	146	19.01	106
Ni-VC$_{3-2}$@C-800	35	101	159	31.68	118
Ni-VC$_{2-1}$@C-800	21	115	163	33.41	142

Figure S5. XRD patterns of samples carbonized 800°C with different Ni incorporation.
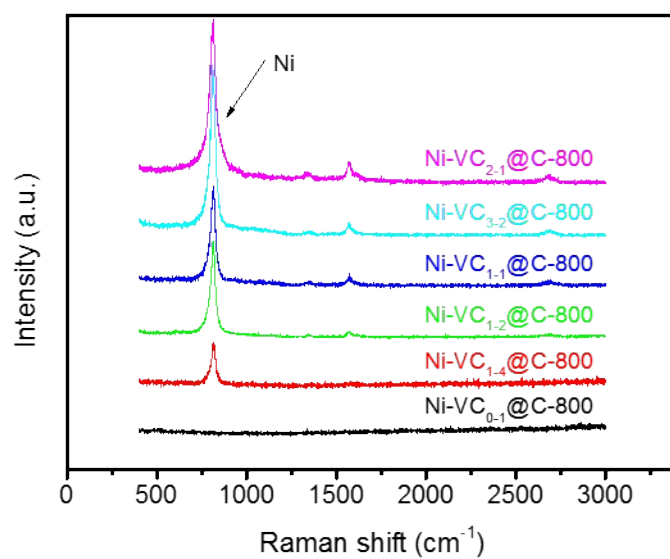

Figure S6. Raman spectrums of samples carbonized 800°C with different Ni incorporation.
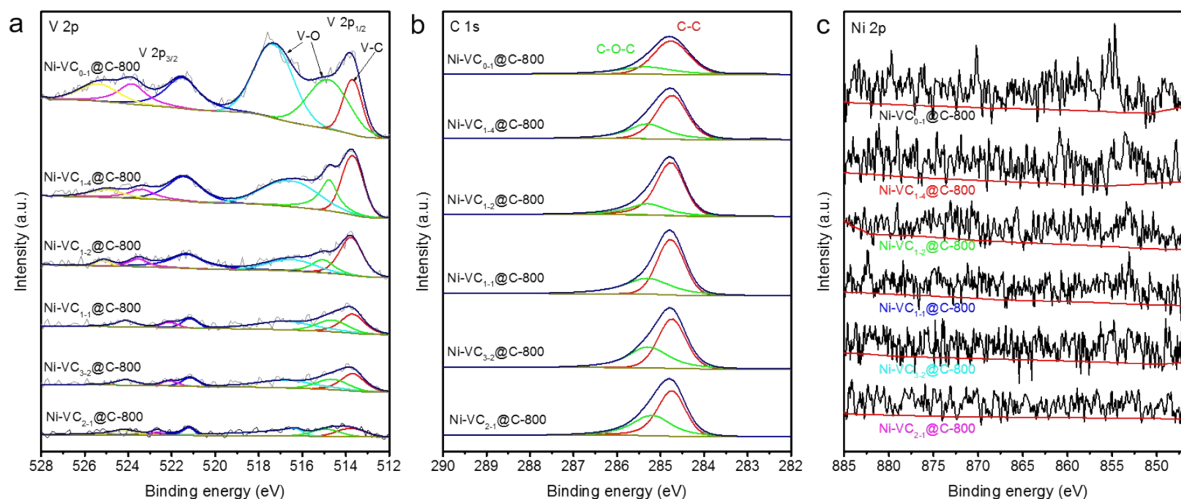
Figure S7. (a) V 2p, (b) C 1s and (c) Ni 2p XPS spectrums of samples carbonized 800°C with different Ni incorporation. The V contents of the precursors before carbonization all stay around 10 at.% and Ni contents increase continuously as the increased addition of Ni salt in the hydrothermal solution.

Table S6. Surface elements contents of samples carbonized 800°C with different Ni incorporation.

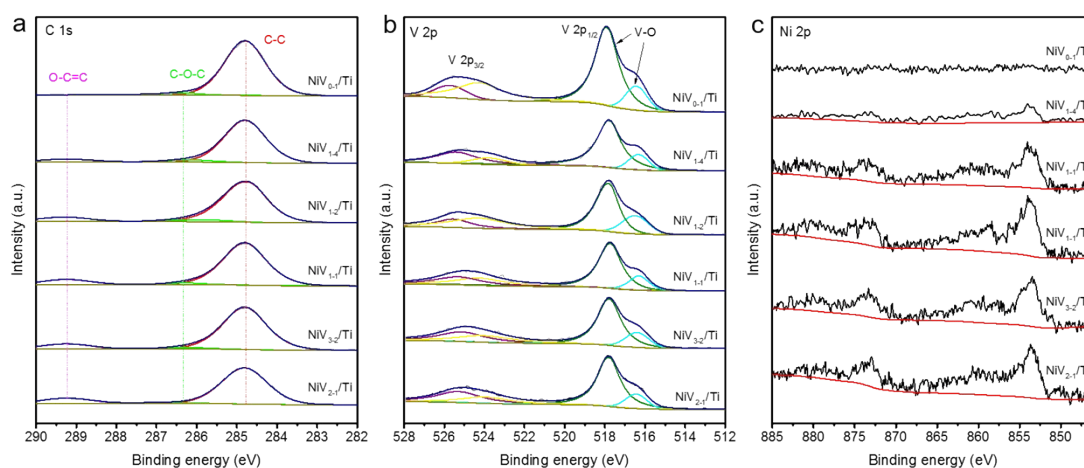| Catalysts	V 2p	Ni 2p[*]	C 1s	O 1s
Ni-VC$_{0-1}$@C-800	5.96	/	80.44	12.16
Ni-VC$_{1-4}$@C-800	3.10	/	90.19	5.24
Ni-VC$_{1-2}$@C-800	1.86	/	95.25	1.91
Ni-VC$_{1-1}$@C-800	0.96	/	95.91	2.22
Ni-VC$_{3-2}$@C-800	0.90	/	94.56	3.67
Ni-VC$_{2-1}$@C-800	0.77	/	94.17	4.16

[*]Below detection limit.

Figure S8. (a) V 2p, (b) C 1s and (c) Ni 2p XPS spectrums of Ni-VO$_2$/Ti precursors with different Ni incorporation.

Table S7. Surface elements contents of Ni-VO$_2$/Ti precursors with different Ni incorporation.

Catalysts	V 2p	Ni 2p	C 1s	O 1s
NiV$_{0-1}$/Ti	13.18	0	46.09	35.57
NiV$_{1-4}$/Ti	10.64	2.85	46.31	36.22
NiV$_{1-2}$/Ti	10.13	3.74	44.71	39.09
NiV$_{1-1}$/Ti	10.16	3.87	45.41	37.49
NiV$_{3-2}$/Ti	9.49	3.87	44.36	39.61
NiV$_{2-1}$/Ti	10.36	4.27	40.96	42.13

Table S8. Summary of Mo-based electrocatalysts for HER in acidic electrolytes.

Catalysts	Mass loading (mg cm^{-2})	media	Onset potential (mV)	Overpotential @10mA/cm^2 (mV)	Tafel slope (mV dec^{-1})	ref
Ni-VC@C nanocabage	0.8	0.5 M H_2SO_4	47	138	61	**This work**
		1 M KOH	35	146	97	
Mo_2C/CNT	2	0.1 M $HClO_4$	64	>150	55.2	1
c-Mo_2C	0.102	1 M KOH	--	293	58	2
γ-Mo_2N	0.102	1 M KOH	--	353	108	2
VC-NS	0.28	0.5 M H_2SO_4	40	98	56	3
WSe_2-C	--	0.5 M H_2SO_4	--	158	98	4
$NiMoN_x$/C	0.25	0.1 M $HClO_4$	~150	--	35.9	5
Co_2P	1	0.5 M H_2SO_4	>70	134	71	6
CoS_2 nanowire	~1.7	0.5 M H_2SO_4	--	145	51.6	7
CoS_2 microwire	~25	0.5 M H_2SO_4	--	158	58	7
Ni_2P	~1	0.5 M H_2SO_4	--	~120	46	8
MoB	2.5	1 M H_2SO_4	--	220	55	9
$CoMoS_3$	0.5	0.5 M H_2SO_4	75	171	57	10

MoCx octahedrons	0.8	0.5 M H_2SO_4	87	142	53	11
		1 M KOH	92	151	59	11
Ni-MoC	0.12	0.5 M H_2SO_4	--	192	98	12
		1 M KOH	--	123	84	12
FeP/C	0.44	0.5 M H_2SO_4	--	71	52	13
WS$_2$ nanoflake	0.35	0.5 M H_2SO_4	--	~150	48	14
Ni$_{12}$P$_5$	3	0.5 M H_2SO_4	--	107	63	15
Hex-WO$_3$	--	1 M H_2SO_4	--	100@33.67mA/cm^2	116	16
W(S$_{0.48}$Se$_{0.52}$)$_2$	0.21	1 M H_2SO_4	--	360@100mA/cm^2	105	17
P$_8$W$_{48}$/rGO	0.3	0.5 M H_2SO_4	--	28	38	18
CoSe$_2$ NP	2.8	0.5 M H_2SO_4	--	139	42.1	19

References:

1. W. F. Chen, C. H. Wang, K. Sasaki, N. Marinkovic, W. Xu, J. T. Muckerman, Y. Zhu and R. R. Adzic, *Energy & Environmental Science*, 2013, **6**, 943-951.

2. L. Ma, L. R. L. Ting, V. Molinari, C. Giordano and B. S. Yeo, *Journal of Materials Chemistry A*, 2015, **3**, 8361-8368.

3. X. Peng, L. S. Hu, L. Wang, X. M. Zhang, J. J. Fu, K. F. Huo, L. Y. S. Lee, K. Y. Wong and P. K. Chu, *Nano Energy*, 2016, **26**, 603-609.

4. M. L. Zou, J. D. Chen, L. F. Xiao, H. Zhu, T. T. Yang, M. Zhang and M. L. Du, *Journal of Materials Chemistry A*, 2015, **3**, 18090-18097.

5. W. F. Chen, K. Sasaki, C. Ma, A. I. Frenkel, N. Marinkovic, J. T. Muckerman, Y. M. Zhu and R. R. Adzic, *Angew Chem Int Edit*, 2012, **51**, 6131-6135.

6. Z. P. Huang, Z. Z. Chen, Z. B. Chen, C. C. Lv, M. G. Humphrey and C. Zhang, *Nano Energy*, 2014, **9**, 373-382.

7. M. S. Faber, R. Dziedzic, M. A. Lukowski, N. S. Kaiser, Q. Ding and S. Jin, *Journal of the American Chemical Society*, 2014, **136**, 10053-10061.

8. E. J. Popczun, J. R. McKone, C. G. Read, A. J. Biacchi, A. M. Wiltrout, N. S. Lewis and R. E. Schaak, *Journal of the American Chemical Society*, 2013, **135**, 9267-9270.

9. H. Vrubel and X. L. Hu, *Angew Chem Int Edit*, 2012, **51**, 12703-12706.

10. L. Yu, B. Y. Xia, X. Wang and X. W. Lou, *Advanced materials*, 2016, **28**, 92-97.

11. H. B. Wu, B. Y. Xia, L. Yu, X. Y. Yu and X. W. Lou, *Nature communications*, 2015, **6**.

12. X. B. Xu, F. Nosheen and X. Wang, *Chemistry of Materials*, 2016, **28**, 6313-6320.

13. D. Y. Chung, S. W. Jun, G. Yoon, H. Kim, J. M. Yoo, K. S. Lee, T. Kim, H. Shin, A. K. Sinha and S. G. Kwon, *Journal of the American Chemical Society*, 2017, **139**, 6669.

14. L. Cheng, W. Huang, Q. Gong, C. Liu, Z. Liu, Y. Li and H. Dai, Angewandte Chemie, 2014, 53, 7860-7863.

15. Z. Huang, Z. Chen, Z. Chen, C. Lv, H. Meng and C. Zhang, ACS nano, 2014, 8, 8121-8129.

16. A. Phuruangrat, J. H. Dong, S. J. Hong, S. Thongtem and J. S. Lee, Journal of Materials Chemistry, 2010, 20, 1683-1690.

17. K. Xu, F. Wang, Z. Wang, X. Zhan, Q. Wang, Z. Cheng, M. Safdar and J. He, *ACS nano*, 2014, **8**, 8468.

18. R. Liu, G. Zhang, H. Cao, S. Zhang, Y. Xie, A. Haider, U. Kortz, B. Chen, N. S. Dalal and Y. Zhao, *Energy & Environmental Science*, 2016, **9**, 1012-1023.

19. D. Kong, H. Wang, Z. Lu and Y. Cui, Journal of the American Chemical Society, 2014, 136, 4897-4900.